ORIGINAL RESEARCH

Platelet GpIbα Binding to von Willebrand Factor Under Fluid Shear: Contributions of the D′D3-Domain, A1-Domain Flanking Peptide and O-Linked Glycans

Sri R. Madabhushi, PhD;* Changjie Zhang, MS;* Anju Kelkar, PhD; Kannayakanahalli M. Dayananda, PhD; Sriram Neelamegham, PhD

***Background*—**Von Willebrand Factor (VWF) A1-domain binding to platelet receptor GpIbα is an important fluid-shear dependent interaction that regulates both soluble VWF binding to platelets, and platelet tethering onto immobilized VWF. We evaluated the roles of different structural elements at the N-terminus of the A1-domain in regulating shear dependent platelet binding. Specifically, the focus was on the VWF D′D3-domain, A1-domain N-terminal flanking peptide (NFP), and O-glycans on this peptide.

***Methods and Results*—**Full-length dimeric VWF (ΔPro-VWF), dimeric VWF lacking the D′D3 domain (ΔD′D3-VWF), and ΔD′D3-VWF variants lacking either the NFP (ΔD′D3NFP^{-}-VWF) or just O-glycans on this peptide (ΔD′D3OG^{-}-VWF) were expressed. Monomeric VWF-A1 and D′D3-A1 were also produced. In ELISA, the apparent dissociation constant (K_D) of soluble ΔPro-VWF binding to immobilized GpIbα ($K_D \approx 100$ nmol/L) was 50- to 100-fold higher than other proteins lacking the D′D3 domain ($K_D \sim 0.7$ to 2.5 nmol/L). Additionally, in surface plasmon resonance studies, the on-rate of D′D3-A1 binding to immobilized GpIbα ($k_{on}=1.8\pm0.4\times10^4$ $(mol/L)^{-1}\cdot s^{-1}$; $K_D=1.7$ μmol/L) was reduced compared with the single VWF-A1 domain ($k_{on}=5.1\pm0.4\times10^4$ $(mol/L)^{-1}\cdot s^{-1}$; $K_D=1.2$ μmol/L). Thus, VWF-D′D3 primarily controls soluble VWF binding to GpIbα. In contrast, upon VWF immobilization, all molecular features regulated A1-GpIbα binding. Here, in ELISA, the number of apparent A1-domain sites available for binding GpIbα on ΔPro-VWF was ≈50% that of the ΔD′D3-VWF variants. In microfluidics based platelet adhesion measurements on immobilized VWF and thrombus formation assays on collagen, human platelet recruitment varied as ΔPro-VWF<ΔD′D3-VWF<ΔD′D3NFP^{-}-VWF<ΔD′D3OG^{-}-VWF.

***Conclusions*—**Whereas VWF-D′D3 is the major regulator of soluble VWF binding to platelet GpIbα, both the D′D3-domain and N-terminal peptide regulate platelet translocation and thrombus formation. **(*J Am Heart Assoc*. 2014;3:e001420 doi 10.1161/JAHA.114.001420)**

Key Words: blood platelets • cell adhesion • microfluidics • thrombosis • von Willebrand factor

Von Willebrand factor (VWF) is a multi-domain plasma glycoprotein that regulates platelet adhesion under fluid shear, both during normal blood coagulation and pathological conditions of arterial occlusion such as myocardial infarction and stroke.[1] VWF is produced in endothelial cells and megakaryocytes. It is secreted into blood as a linear polymer composed of ≈0.5 megadalton (MDa) dimer/protomer repeat units. The primary structure of VWF consists of various domain-assemblies arranged in the sequence D′D3-A1-A2-A3-D4 followed by 6 C-type and the CK structures.[2]

VWF binding to platelet GpIbα is promoted by hydrodynamic shear and it occurs under 2 scenarios: (1) Soluble VWF binds platelet GpIbα under abnormally high fluid shear stress conditions that can occur in stenosed vessels and prosthesis (including heart valves and left ventricular assist devices).[3–5] This binding involves recognition of soluble VWF A1-domain by platelet GpIbα. (2) VWF immobilized on extracellular matrix components like collagen exposed on the denuded vascular endothelium can form a molecular bridge to capture platelets.[6,7] Such binding contributes to thrombus growth. Here, the VWF A3-domain primarily binds matrix proteins with the A1-domain capturing platelets. The precise mechanism by which the interplay between fluid flow and protein structure regulates VWF-GpIbα molecular binding in these 2 cases remains unresolved.

From the Department of Chemical and Biological Engineering and The NY State Center for Excellence in Bioinformatics and Life Sciences, State University of New York, Buffalo, NY.

*Dr Madabhushi and Dr Zhang contributed equally.

Accompanying Figures S1 through S7 and Movie S1 are available at http://jaha.ahajournals.org/content/3/5/e001420/suppl/DC1

Correspondence to: Sriram Neelamegham, PhD, 906 Furnas Hall, State University of New York, Buffalo, NY 14260. E-mail: neel@buffalo.edu
Received September 5, 2014; accepted September 25, 2014.

A number of recent studies provide evidence that the interaction between neighboring domains of VWF regulates its functions, including the binding between VWF-A1 and platelet GpIbα.[8–11] Specifically, based on the co-crystal containing VWF-A1 and GpIbα, Huizinga et al[12] propose that the N- (amino acids/aa 1261 to 1271) and C-terminal (aa1459 to 1468) "flanking peptides" of VWF-A1 may hinder VWF-GpIbα binding. In support of this, both peptides lie close to the GpIbα binding interface called "β-finger" in unliganded VWF-A1 with substantial peptide displacement being noted in the VWF-GpIbα complex. In addition to the peptide rearrangement, Dumas et al[13] show that additional structural features also differ between unliganded and GpIbα-liganded VWF-A1. This includes substantial changes in the VWF α1β2-loop and additional differences in the residues interacting with Arg^{571}. Functional data supporting a role for the "VWF-A1 *N*-terminal *f*lanking-*p*eptide" (abbreviated NFP) in regulating VWF-GpIbα binding has been reported.[8,14] Here, the inclusion of the peptide Gln^{1238}-Glu^{1260} at the N-terminus of VWF-A1 in the A1-A3 tri-domain construct reduced platelet accumulation on VWF immobilized on fibrinogen.[8] Addition of the synthetic non-glycosylated Gln^{1238}-Glu^{1260} peptide also reduced platelet recruitment on immobilized VWF.[14] In addition to the NFP, Ulrichts et al[11] proposed that the VWF-D′D3-domain may shield A1-GpIbα binding interactions.[11] While their experiments evaluated the role of the D′D3-domain when ristocetin was agonist, the impact of VWF-D′D3 in the presence of fluid shear was not examined. Further, 2 different recombinant VWF proteins were utilized, one N-terminal dimerized molecule containing VWF D′D3-A3 (aa764 to 1874) and a second C-terminal dimerized protein that lacks both VWF-D′D3 and the NFP (aa1260 to 2813). Thus, the relative contributions of VWF-D′D3 and NFP were not determined. In addition to the above, the NFP potentially contains 4 O-glycans at Thr^{1248}, Thr^{1255}, Thr^{1256}, and Ser^{1263}[15] and these carbohydrates may influence VWF-A1 GpIbα binding.[16,17] Overall, while accumulating evidence suggests that the amino acids at the N-terminus of VWF-A1 regulate GpIbα binding, the precise contributions of the D′D3-domain, NFP, and the O-glycans on the NFP remains unknown. Such analysis is nevertheless important since it is not possible to understand the absolute importance of any particular structural feature on cell adhesion function, without considering the impact of competing elements under identical experimental conditions.

Here, we analyzed the relative contributions of different structural features at the N-terminus of VWF-A1 on both the binding of soluble VWF to platelets and the capture of platelets from flow. To this end, a systematic set of molecules based on either dimeric VWF or single VWF domains was generated. ELISA, microfluidics based platelet adhesion and thrombus formation assays, and surface plasma resonance (SPR) based experiments were undertaken. The results demonstrate that multiple structural features at the N-terminus of VWF-A1 regulate platelet adhesion under hydrodynamic shear, with the D′D3 domain playing a dominant role under all experimental condition.

Methods

Dimeric VWF Variant Expression

Dimeric full-length VWF (ΔPro-VWF, aa764 to 2813, ≈500 kDa), dimeric VWF lacking the D′D3 domain (ΔD′D3-VWF, aa1243 to 2813, ≈400 kDa), ΔD′D3-VWF lacking the NFP (ΔD′D3NFP^{-}-VWF, aa1267 to 2813, ≈400 kDa), and ΔD′D3-VWF with Ala mutations replacing Thr/Ser (ΔD′D3OG^{-}-VWF, aa1243 to 2813 with T1248A, S1253A, T1255A, and T1256A, ≈400 kDa) were expressed by transient transfection of HEK293T cells and purified by ion exchange chromatography.[18]

To express the above proteins, a vector encoding for dimeric full-length VWF (ΔPro-VWF, amino acid 764 to 2813) was available from a previous study.[19] This is identical to full-length VWF only it lacks the VWF propeptide 1 to 763. An additional dimeric protein, ΔD′D3-VWF (amino acid 1243 to 2813) that lacks the D′D3 domain, was generated by PCR amplifying VWF amino acids 1243 to 2813. The resulting product replaced the single D′D3 domain in the vector "pCSCG-SS-KZK-D′D3-FLAG-His".[9] ΔD′D3OG^{-}-VWF was constructed by restriction digestion of the ΔD′D3-VWF plasmid with *AgeI* and *Pf1FI* (Tth111I). The excised 111 bp fragment was replaced with a 111 bp synthetic double-stranded DNA containing overhangs complementary to *AgeI* and *Pf1FI* enzymes sites, as described below. Single base substitutions were made such that Thr at positions 1248, 1255, and 1256, and Ser at position 1253 were replaced by Ala. The 111 bp synthetic double-stranded DNA insert was assembled by annealing and ligating 2 pairs of oligonucleotides with complementary overhangs. The pairs of oligonucleotides used during this step were: Oligo 1: 5′ *CCGG*TCTGGTGGTG CCTCCCGCAGATGCCCCGGTGGCCCCCGCCGCTCTGT-ATGTG 3′ annealed with Oligo 1C: 5′ [Phos] GTCCTCCACATACA GAGCGGCGGGGGCCACCGG-GGCATCTGCGGGAGGCACCAC-CAGA 3′, and Oligo 2: 5′ [Phos] GAGGACATCTCGGAACCGC-CGTTGCACGATTTCTACTGCAGCAGGCTACTGGACC 3′ annealed with Oligo 2C: 5′*A*GGTCCAG-TAGCCTGCTGCAGTAGAAATCG TGCAACGGCGGTTCCGAGAT 3′. The ligated oligomer (111 bp) product was gel purified and then inserted into the above ΔD′D3-VWF vector.

Similar to the strategy used to create ΔD′D3OG^{-}-VWF, ΔD′D3NFP^{-}-VWF was made by replacing the 111 bp *AgeI-Pf1FI* fragment of ΔD′D3-VWF with an annealed pair of synthetic oligonucleotides (Oligo 3: 5′ *CCGG*-TTTGCACGATTT CTACTGCAGCAGGCTACTGGACC 3′ and Oligo 3C:5′ *A*-GGT CCAGTAGCCTGCTGCAGTAGAAATCGTGCAAA 3′) containing

base overhangs for cloning into *AgeI/Pf1FI* enzyme sites. The result of this substitution was a protein that lacked amino acids up to 1266 at the N-terminus of the VWF-A1 domain.

Dimeric ΔPro-VWF, ΔD′D3-VWF, ΔD′D3NFP¯-VWF, and ΔD′D3OG¯-VWF were expressed in mammalian cells by transient transfection using the calcium phosphate method.[18] All proteins were purified using Fractogel® EMD TMAE (M) (EMD Millipore, Gibbstown, NJ) and FPLC.[19] Here, the column was first equilibrated with 20 mmol/L Tris buffer, pH 7.4. Cell culture supernatant containing VWF variants was diluted 1:1 in 20 mmol/L Tris buffer (final pH 7.2), and this was run through the column. Following binding, VWF was eluted using 20 mmol/L Tris buffer by increasing NaCl concentration in a stepwise manner from 50 to 100, 200, and finally 400 mmol/L NaCl. Dimeric VWF variants typically eluted at 200 and 400 mmol/L NaCl. Relevant fractions containing proteins were pooled and concentrated using a 50-kDa cutoff centrifugal device (Millipore).

Single Domain VWF and GpIbα-Fc Fusion Proteins

VWF domain constructs, VWF-A1 (aa1243 to 1480, 31 kDa) and D′D3-A1 (aa764 to 1480, 85 kDa) and GpIbα-Fc fusion protein containing aa1 to 290 of GpIbα (130 kDa) were stably expressed in CHO (Chinese Hamster Ovary) cells using lentivirus. These proteins were His-tag purified. Here, cDNA corresponding to the D′D3-A1 (amino acid 764 to 1480) region of VWF was amplified from VWF cDNA using 5′-CGCG CGG*ACCGGT*AGCCTATCCTGTCGGCCCCCCATG-3′ forward primer containing an *Age*I site and 5′- [Phos] *AAC*CGGGCCC ACAGTGACTTGTGCCATG-3′ reverse primer containing a partial *Hpa*I site. This product replaced VWF-D′D3-FLAG in the vector "pCSCG-SS-KZK-D′D3-FLAG-His"[9] to give "pCSCG-SS-KZK-D′D3-A1-His". The A1-domain was similarly constructed by amplifying DNA corresponding to VWF aa1243 to 1480.

cDNA corresponding to the first 290 amino acids of GpIbα was PCR amplified from the GpIbα-cDNA (Thermo-Scientific/OpenBiosystems, Rockford, IL) using 5′-TTGCAT*AAGCTT*CACCCCATCTGTGAGGTCT-3′ forward primer containing a *Hind*III site and 5′- AGTAT*GGATCC*ACGCACCTTATCGCCCTCAGT-3′ reverse primer containing a *Bam*HI site. The PCR product was cloned into a pCSCG vector prior to cDNA encoding for human IgG1 Fc. The entire segment encoding for the GpIbα-Fc fusion protein was then PCR amplified using 5′–GCTAAT*ACCGGT*CACCCCATCTGTGAGGTCT-3′ forward primer containing an *Age*I site and 5′–ATCATT*TTCGAA*TTTACCCGGAGACAGGGA GAGGC-3′ reverse primer containing a *BstBI* site, and this product replaced VWF-D′D3-FLAG in the vector "pCSCG-SS-KZK-D′D3-FLAG-His".[9] This final plasmid, which expresses the first 290 amino acids of GpIbα followed by a human Fc and $(his)_6$ tag, is called "pCSCG-GpIbα-Fc-His".

Lentivirus transduced stable CHO cell lines were generated to express various individual VWF domains and the GpIbα-Fc chimeric protein.[9] These proteins were secreted into culture medium at 5 to 12 μg/mL, and purified using an AKTA FPLC system and HisTrap HP column (GE Healthcare, Piscataway, NJ) following manufacturer's instructions.

Multimeric human plasma VWF (pVWF) was purified from plasma cryoprecipitate.[20]

Protein Concentration Determination and Gel Electrophoresis

All protein concentrations were determined using the Coomassie/Bradford protein assay kit (Thermo-Pierce, Rockford, IL) or a flow cytometry bead assay.[19] VWF concentration estimates obtained using these methods are within ≈6% of the absolute protein concentration determined using quantitative amino acid analysis.[19] SDS-PAGE (4% to 6% discontinuous gel) followed by Western blotting was performed for characterizing dimeric proteins under non-reducing conditions. Western blots were probed with rabbit polyclonal anti-VWF antibody (Dako, Carpinteria, CA) and detected by HRP conjugated goat anti-rabbit-IgG. Silver staining of some of the gels was performed using a kit from Thermo-Pierce. Similar analysis of other VWF/GpIbα-Fc proteins was performed following 4% to 20% gradient SDS-PAGE under standard reducing conditions.

ELISA

In some runs, 4 μg/mL GpIbα-Fc was adsorbed overnight onto 96-well MaxiSorp plates at 4°C. The wells were then blocked using 30 mmol/L "standard" HEPES buffer (30 mmol/L 4-(2-hydroxyethyl)-1-piperazineethanesulfonic acid, 110 mmol/L NaCl, 10 mmol/L KCl, 1 mmol/L $MgCl_2$, 10 mmol/L Glucose, pH7.4) containing 3% BSA for 2 hour at RT. VWF proteins, at various concentrations, were added to the wells for 1 hour at RT. In some cases, during this incubation step, either 1.5 mg/mL ristocetin or 20 μg/mL anti-GpIbα blocking mAb AK2 was present. Following extensive washing using TBST (Tris-Buffered Saline with 0.1% Tween 20), polyclonal rabbit anti-VWF antibody (Dako) was added to the wells. Bound VWF was detected using HRP conjugated mouse anti-rabbit antibody (Jackson Immuno, West Grove, PA). Dissociation constants (K_D) were estimated using Scatchard analysis.

In other runs, similar to the above, 4 μg/mL VWF proteins were adsorbed overnight onto 96-well MaxiSorp plates at 4°C. Following blocking with BSA, the binding of GpIbα-Fc to immobilized VWF was measured using a HRP conjugated goat anti-human IgG, either in the absence or presence of 1.5 mg/mL ristocetin and/or 20 μg/mL anti-GpIbα mAb AK2.

Equivalent adsorption of all VWF protein variants to the ELISA wells was verified using the polyclonal rabbit anti-VWF antibody (Dako).

Surface Plasmon Resonance (SPR)

SPR studies were conducted using the SR7500DC SPR system (Reichert Technologies, Buffalo, NY) and planar polyethylene glycol/carboxyl sensor chip.[9] Anti-human IgG antibody (Jackson Immuno) was covalently coupled onto the active cell using carbodiimide chemistry. Following this, both the active and reference cells were blocked with BSA. Subsequent perfusion with 30 μg/mL GpIbα-Fc for 5 minutes lead to 300 RU protein captured on the active flow cell and negligible protein immobilization on the reference. Fifty to 1600 nmol/L VWF-A1 or D′D3-A1 in 25 mmol/L HEPES containing 150 mmol/L NaCl, 1.5 mmol/L $CaCl_2$ and 0.01% Tween-20 were then perfused at 15 μL/min with a 3 minutes association phase followed by a 5 minutes dissociation phase. Regeneration was not necessary since VWF domains completely dissociated over 5 minutes. To confirm binding specificity, in some runs, 50 μg/mL anti-GpIbα mAb AK-2 (Millipore, Billerica, MA) was added to immobilized GpIbα-Fc 5 minutes prior to domain perfusion. A1-GpIbα interaction data was processed and analyzed using a simple 1:1 interaction model using Scrubber2 (kindly provided by David Myszka, University of Utah, Salt Lake City).[9]

In some cases, the non-function blocking anti-VWF antibody AVW-1 was immobilized on the SPR sensor surface. ΔPro-VWF or ΔD′D3-VWF were then captured onto these substrates via AVW-1 at comparable levels. GpIbα-Fc was then perfused at different concentrations for 5 minutes prior to the dissociation phase.

Shear Induced Platelet Aggregation (SIPA)

Human blood was drawn in sodium citrate. PRP and Platelet Poor Plasma (PPP) were prepared. PRP was labeled with anti-CD31 PerCP-efluor710 mAb (eBioscience, San Diego, CA) and diluted using PPP to obtain a platelet count of $\approx 10^8$/mL. In some cases, this mixture was incubated with 100 μg/mL anti-VWF-D′D3 mAbs (DD3.1 or DD3.3)[9] or 20 μg/mL anti-VWF-A1 domain mAb AVW-3 for 10 minutes at RT. Platelets were then sheared in a cone-plate viscometer at 9600 s^{-1} as described previously,[4] in the presence or absence of agonist, either 0.5 μmol/L adenosine diphosphate (ADP) or 5 μmol/L thrombin receptor activating hexapeptide (TRAP-6). Five microliter samples withdrawn at various times were read using a FACSCalibur flow cytometer for fixed amounts of data acquisition time. Percent platelet aggregation was quantified based on the loss of single platelets.

Flow Chamber Studies

Human subject protocols were approved by the SUNY-Buffalo Institutional Review Board. Blood was obtained from healthy human adult volunteers by venipuncture into a syringe containing 1:9 of 3.8% sodium citrate and 2 μmol/L prostaglandin E-1. The blood was centrifuged at 240*g* for 15 minutes to obtain platelet rich plasma (PRP). Washed platelets were obtained by further centrifuging the PRP at 1800*g* for 7 minutes and resuspending the platelet pellet in standard HEPES buffer.

For cell adhesion studies, a 1×1 mm region of a 100 mm tissue culture petri dish was incubated with 20 μg/mL VWF variants or pVWF overnight at 4°C. Equivalent amounts of protein were adsorbed as confirmed by ELISA. The surface was then blocked with HEPES buffer containing 1% BSA for 1 hour at RT. A custom PDMS (polydimethylsiloxane) microfluidic flow cell (400 μm width×100 μm height×1 cm length) was vacuum sealed onto the VWF substrate and the apparatus was mounted on a Zeiss AxioObserver microscope (Thornwood, NY).[18] Washed platelets ($\approx 10^8$/mL) were perfused on immobilized VWF at wall shear stress ranging from 1 to 20 dyn/cm^2. Images were acquired at 10 frames per second using a pco.edge sCMOS camera (Kelheim, Germany). Platelet accumulation and translocation velocity were quantified using NIH ImageJ. Here, platelet accumulation (cells/mm^2) quantifies the number of substrate bound platelets 2 minutes after the initiation of perfusion. Platelet translocation velocity (μm/s) quantifies the distance moved by platelets in a 5-second interval.[21]

For the thrombus formation assay, washed erythrocytes were obtained. To this end, the packed red blood cells remaining after PRP isolation were resuspended in equal volume of normal saline and repeatedly washed 3 to 4 times to remove residual plasma and buffy coat components. In the final step, the erythrocytes were resuspended in standard HEPES buffer. 10^8 washed platelets/mL (final concentration) labeled with 2 μmol/L BCECF-AM (2′,7′-bis-(2-carboxyethyl)-5-(and-6)-carboxyfluorescein, acetoxymethyl ester) were added to erythrocytes at 50% hematocrit along with 10 μg/mL VWF variants. This suspension was then perfused in the microfluidic flow chamber that was coated overnight with 20 μg/mL equine fibrillar collagen type I (Chrono-log Corp, Havertown, PA) at 100 to 1000/s (wall shear stress ≈4 to 40 dyn/cm^2) for 5 minutes. Images were captured at 5-second intervals. Thrombus formation was quantified, using ImageJ software, as the percent of the collagen surface in the field of view that was occupied by platelets.

All studies with human blood were performed with 4 human donors under each experimental condition.

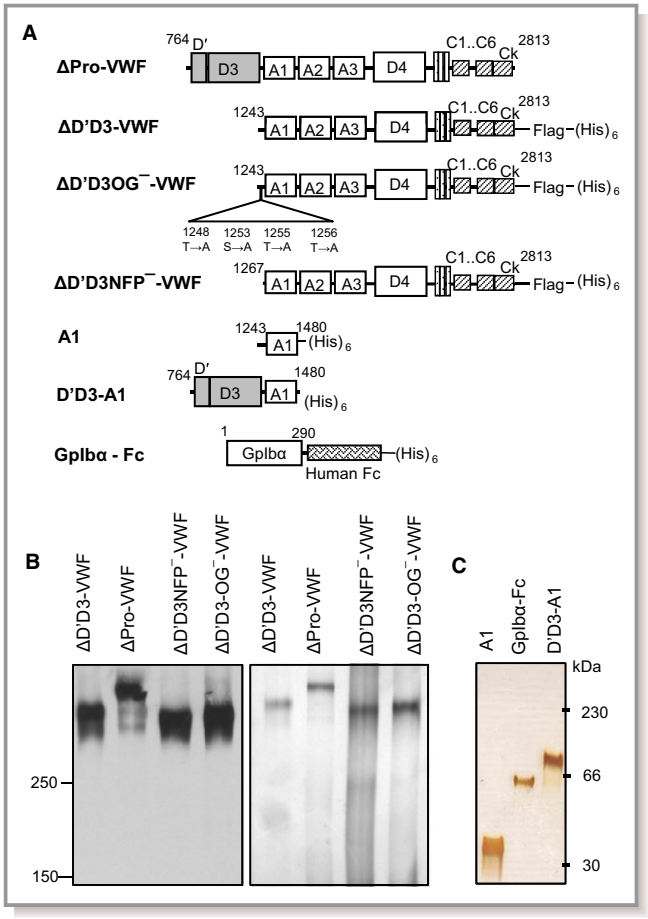

Figure 1. Overall schematic. A, Representation of VWF dimeric protein constructs (ΔPro-VWF, ΔD′D3-VWF, ΔD′D3OG⁻-VWF and ΔD′D3NFP⁻-VWF), monomeric VWF domains (A1 and D′D3-A1) and GpIbα-Fc fusion protein. B, Left panel shows western blot of dimeric VWF protein variants under non-reducing condition, probed with rabbit polyclonal anti-human VWF antibody. Right panel shows same proteins in silver stained gel. C, Silver stain of monomeric domain proteins and GpIbα-Fc. NFP indicates N-terminal flanking peptide; OG, O-glycans; VWF, Von Willebrand Factor.

Statistics

Experimental data are presented as mean±SD for ≥3 experiments. Student *t* test (2-tailed) was performed for dual comparisons. ANOVA followed by the Tukey post-test was applied for multiple comparisons. $P<0.05$ was considered significant.

Results

Systematic Panel of Recombinant Proteins

This study compared the relative roles of different VWF structural features on platelet adhesion and thrombus formation. Two series of recombinant proteins were expressed (Figures 1A and S1). First, C-terminal dimerized full-length VWF variants were produced since single VWF domains do not reproduce the complex behavior of the entire molecule. Studies using multimeric VWF variants are also complex to interpret due to the heterogeneous nature of protein multimerization. The proteins expressed include full-length dimeric VWF with intact D′D3-domain (ΔPro-VWF), a variant lacking the D′D3-domain but with the VWF-A1 NFP (ΔD′D3-VWF), a construct lacking both the D′D3-domain and NFP (ΔD′D3NFP⁻-VWF) and a mutant where the O-glycans in the flanking-peptide were replaced by Ala (ΔD′D3OG⁻-VWF). The molecular mass and purity of these proteins is shown (Figure 1B). Second, the monomeric VWF-A1 domain with the flanking-peptide, the D′D3-A1 domain and the GpIbα-Fc fusion protein were obtained at >90% purity (Figure 1C). While details are provided in the following sections, the Table summarizes the results from functional studies performed using the above constructs.

Soluble VWF With D′D3-Domain Deletion Binds GpIbα Even in the Absence of Ristocetin

The binding of soluble VWF to immobilized GpIbα-Fc was measured since this can occur on platelets under high fluid shear conditions.[4,20] In ELISA, all constructs lacking the D′D3-domain (ΔD′D3-VWF, ΔD′D3NFP⁻-VWF and ΔD′D3OG⁻-VWF) bound GpIbα avidly in the absence of ristocetin (Figure 2A). The apparent K_D of ΔPro-VWF binding to GpIbα-Fc (K_D=102 nmol/L) was 50- to 100-fold higher compared with the constructs that lack the D′D3 domain (K_D=0.7 to 2.4 nmol/L) (Figure S2). The O-glycans at the N-terminus had no significant effect since ΔD′D3-VWF and ΔD′D3OG⁻-VWF displayed similar binding. ΔD′D3NFP⁻-VWF exhibited enhanced binding to GpIbα-Fc (K_D=0.7 nmol/L) compared with ΔD′D3⁻-VWF (K_D=2.4 nmol/L) suggesting a small but significant role for the NFP in regulating VWF-A1 GpIbα binding function.

Addition of 1.5 mg/mL ristocetin enhanced binding of all VWF-variants to GpIbα-Fc except ΔD′D3NFP⁻-VWF, in which case ristocetin was inhibitory (Figures 2B and S3). The increased binding of ΔD′D3-VWF and ΔD′D3OG⁻-VWF to GpIbα-Fc upon ristocetin addition is expected since these proteins harbor the full ristocetin binding site, at both the N-terminus (aa1238 to 1251) and C-terminus (aa1459 to 1472) of the A1-domain.[22,23] The inhibition of binding in the case of ΔD′D3NFP⁻-VWF is unexpected but robustly reproducible. Here, ristocetin may block A1-GpIbα binding in the absence of the N-terminal residues.

In controls, the binding of VWF variants to immobilized GpIbα-Fc was blocked by anti-GpIbα mAb AK-2, in the absence and presence of ristocetin (Figure 2C). No binding was observed in BSA coated wells or wells bearing isotype

Table. Summary of Results*

	Description	VWF Binding to Immobilized GpIbα-Fc†	GpIbα-Fc Binding to Immobilized VWF (Static)†	Platelet Binding to Immobilized VWF (Shear)‡
Dimeric VWF constructs:				
Pro-VWF	Dimeric VWF	+/− (K_D=102 nmol/L)	+ (K_D=15 nm, 50% active)	+/−
ΔD'D3-VWF	Lacks D'D3 domain	++ (K_D=2.4 nmol/L)	++ (K_D=9 nmol/L)	++
ΔD'D3NFP¯-VWF	Lacks D'D3 and N-terminal peptide	+++ (K_D=0.7 nmol/L)	++ (K_D=7 nmol/L)	+++
ΔD'D3OG¯-VWF	Lacks D'D3 and O-glycans on N-terminal peptide	++ (K_D=2.4 nmol/L)	+++ (K_D=5 nmol/L)	++++
Monomeric constructs:				
A1	A1 domain with N-terminal peptide	High on-rate: 5×10^4 $(mol/L)^{-1}\cdot s^{-1}$	N.D. (multivalent)	N.D.
D'D3-A1	2 domains together	Low on-rate: 1.8×10^4 $(mol/L)^{-1}\cdot s^{-1}$	N.D. (multivalent)	N.D.

NFP indicates N-terminal flanking peptide; OG, O-glycans; SPR, surface plasma resonance; VWF, Von Willebrand Factor.
*+/− nomenclature is used to qualitatively indicate apparent binding in various assays. +/−: weak binding; + : measurable but low binding; ++: significant binding; +++ and ++++: highest binding.
†ELISA was performed for dimeric VWF and SPR for single domain constructs. SPR studies with dimeric VWF or GpIbα-Fc in solution were not performed since these constructs are multivalent. ELISA studies were not performed with single domain constructs due to their high binding on- and off-rates.
‡Summary of both platelet translocation and thrombus formation assays.

control, P-selectin glycoprotein ligand-1 Fc fusion protein.[24] Overall, soluble VWF binding to platelet GpIbα is primarily inhibited by VWF-D'D3 with the N-terminal peptide having a smaller contribution.

Binding of A1 and D'D3-A1 to GpIbα-Fc

The above ELISA studies suggest fundamental differences in the nature of GpIbα binding to VWF-A1 in the absence or presence of coupled D'D3. To test this, the binding of monomeric VWF-A1 and D'D3-A1 to immobilized GpIbα-Fc was evaluated using SPR (Figure 3). Here, the single A1-domain bound GpIbα-Fc with a rapid on-rate ($5.05\pm0.4\times10^4$ $(mol/L)^{-1}\cdot s^{-1}$) and a dissociation constant (K_D) of 1.2±0.3 μmol/L (Figure 3A). In comparison, D'D3-A1 displayed a slower on-rate ($1.79\pm0.4\times10^4$ $(mol/L)^{-1}\cdot s^{-1}$) and comparable K_D of 1.7±1 μmol/L (Figure 3B). The measured binding was specific as this was blocked by mAb AK-2 (Figure 3C). While the data in Figure 3A were fit well by the 1:1 binding model, this was not the case in Figure 3B particularly during the dissociation phase after 3 minutes. Inverse experiments where GpIbα-Fc in solution bound immobilized VWF-A1 and D'D3-A1 are not presented since this results in bivalent binding that is not well suited for SPR studies. Overall, the slower on-rate of D'D3-A1 binding to GpIbα-Fc compared with A1-GpIbα interaction supports the notion that the VWF D'D3-domain attenuates VWF-A1 binding. Further, the inability to fit all binding data to a simple single-site interaction model suggests that beyond simple steric hindrance or "shielding," the interaction between D'D3-A1 and GpIbα is likely more complex.

Anti-D'D3 mAb DD3.1 Inhibits Platelet Aggregation

The proposition that the D'D3-domain reduces VWF-A1 function was tested in shear induced platelet aggregation (SIPA) studies that utilized full length endogenous multimeric plasma VWF (Figure 4). In these viscometer studies, SIPA at 9600 s^{-1} was completely inhibited both by an anti VWF-A1 mAb AVW-3 and an anti VWF-D'D3 mAb DD3.1 (Figure 4A). Isotype control anti-VWF-D'D3 mAb DD3.3 did not alter SIPA. Partial inhibition (≈50%) of platelet aggregation by mAb DD3.1 was also noted in the presence of the agonists ADP (Figure 4B) and TRAP-6 (Figure 4C) when the shear rate was 9600 s^{-1}. Blocking in these panels was not complete, due to the extremely high levels of platelet aggregation (≈90% within 20 seconds) initiated by the agonists. Overall, since an anti-D'D3 mAb inhibits VWF-A1 function, the spatial proximity of VWF-D'D3 and -A1 may have important consequences on multimeric VWF-platelet binding under fluid shear.

Lower Binding of Immobilized ΔPro-VWF to GpIbα Compared to Other Constructs

VWF variants were immobilized in order to mimic conditions where platelets from flow are captured at sites of vascular injury. In ELISA, all proteins lacking the D'D3-domain bound GpIbα-Fc at higher affinity compared to ΔPro-VWF: ΔPro-VWF (K_D=15.1 nmol/L)<ΔD'D3-VWF (9.6 nmol/L)≈ΔD'D3NFP¯-VWF (7.5 nmol/L)<ΔD'D3OG¯-VWF (4.9 nmol/L) (Figures 5 and S4). Here, at the highest GpIbα-Fc concentration, the extent of ΔPro-VWF binding was half that of the other

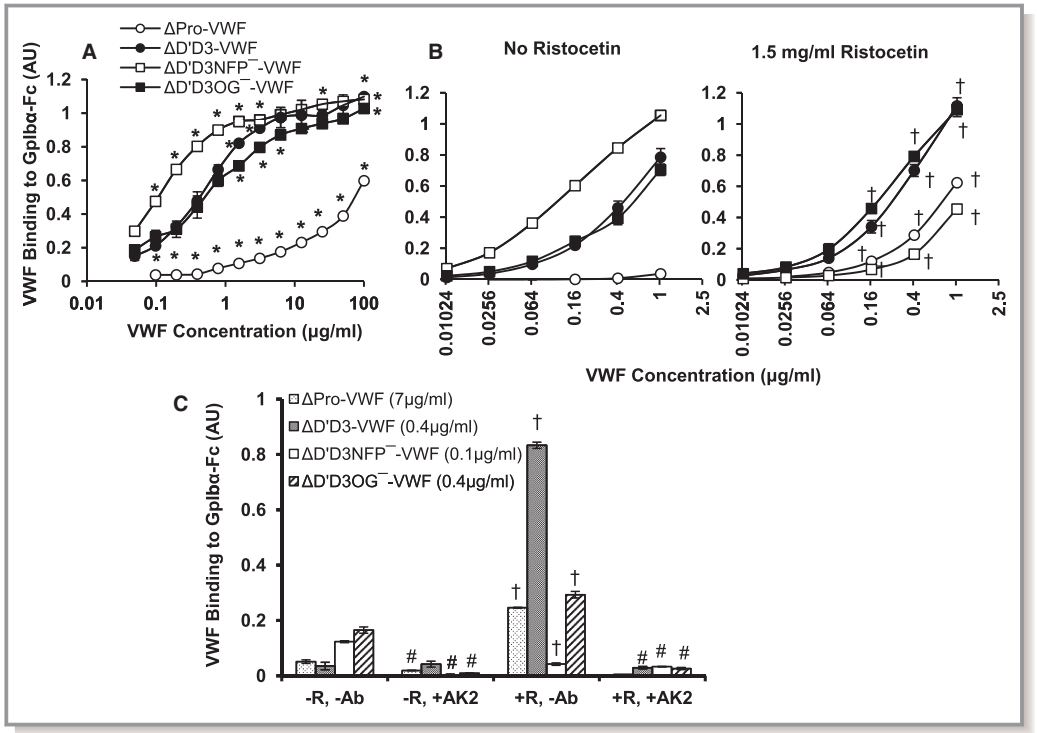

Figure 2. ELISA measurement of VWF binding to immobilized GpIbα-Fc. 4 μg/mL GpIbα-Fc was immobilized in the wells overnight. VWF dimeric protein variants were added in the absence or presence of ristocetin. A, VWF protein variant (0.05 to 100 μg/mL) binding to immobilized GpIbα-Fc in the absence of ristocetin. K_D values were estimated using Scatchard analysis (see Figures S1 through S7). B, VWF variants binding to immobilized GpIbα-Fc in the absence and presence of 1.5 mg/mL ristocetin. C, VWF variant proteins were added at their K_D concentrations to wells containing immobilized GpIbα-Fc in the absence or presence of 1.5 mg/mL ristocetin (−R or +R) or 20 μg/mL blocking antibody (−AB=no blocking antibody; +AK2=anti-GpIbα antibody AK2). *, † and # denote $P<0.05$ with respect to all other treatments (A), no ristocetin treatment (B and C) and no blocking antibody control (C), respectively. Data are representative of 3 to 4 independent runs with each run having 2 to 3 repeats. Error bars are too small to be visible in many cases. All analysis was performed using ANOVA separtely for each concentration. ANOVA indicates analysis of variance; NFP, N-terminal flanking peptide; OG, O-glycans; VWF, Von Willebrand Factor.

mutants. Thus, upon immobilization, ΔPro-VWF may adopt a conformation where only a portion of its A1-domain is available for GpIbα binding. ΔD′D3OG⁻-VWF exhibited higher binding compared to all other molecules suggesting a role for the O-glycans during this interaction.

Similar to ELISA, SPR experiments were performed where either ΔPro-VWF or ΔD′D3-VWF was captured on the sensor surface via an anti-VWF mAb. Different concentrations of GpIbα-Fc were then perfused (Figure S5). Here, a concentration-dependent binding response was only observed for GpIbα-Fc binding to immobilized ΔD′D3-VWF. GpIbα-Fc binding to ΔPro-VWF was low.

Addition of 1.5 mg/mL ristocetin improved the binding of GpIbα-Fc to all immobilized VWF constructs. The effect on ΔD′D3OG⁻-VWF was small since this protein displayed maximal binding even prior to ristocetin addition (Figures 5B and S6). GpIbα-Fc bound all VWF variants with similar affinities upon ristocetin addition (Figure 5B). Anti-GpIbα mAb AK-2 blocked GpIbα-VWF binding under all conditions (Figure 5C). Together, the data suggest an important role for the VWF-D′D3 domain in regulating GpIbα binding with additional contributions from the O-glycans on the NFP.

Role for Both the D′D3 Domain and NFP in Regulating Platelet Translocation

Washed human platelet capture and translocation on physisorbed ΔPro-VWF, ΔD′D3-VWF, ΔD′D3NFP⁻-VWF, ΔD′D3OG⁻-VWF and pVWF was assayed using a microfluidic flow device at physiological shear stresses from 1 to 20 dyn/cm^2. Equivalent amounts of VWF were immobilized in each case (data not shown). Here, at 1 dyn/cm^2, significant platelet accumulation was observed on ΔD′D3-VWF, ΔD′D3NFP⁻-VWF, and ΔD′D3OG⁻-VWF but not ΔPro-VWF or pVWF (Figure 6A, Movie S1). At higher shears (3 to 20 dyn/cm^2), a greater number of platelets also translocated

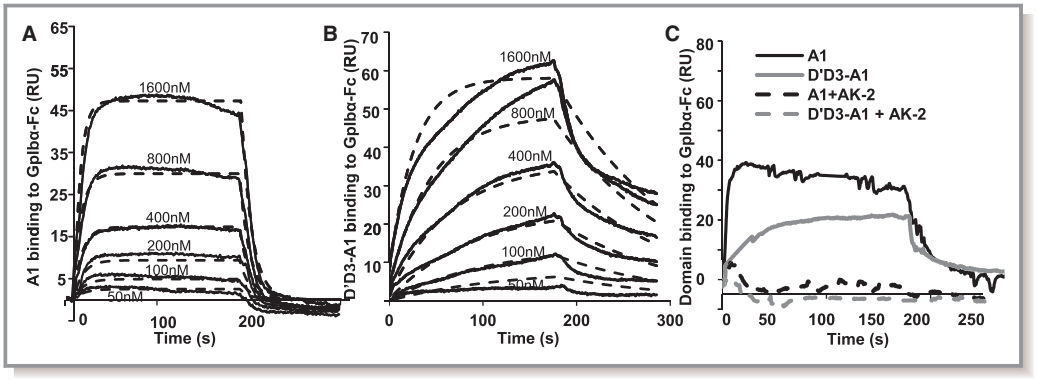

Figure 3. Kinetics and affinity of A1 and D′D3-A1 binding to immobilized GpIbα-Fc. 300 RU GpIbα-Fc was immobilized on the SPR sensor via covalently coupled anti-human IgG. Different concentrations (50 to 1600 nmol/L) of A1 (A) and D′D3-A1 (B) were perfused over the substrate in 25 mmol/L Hepes (pH 7.4) buffer containing 150 mmol/L NaCl, 1.5 mmol/L $CaCl_2$ and 0.01% Tween-20. The kinetic data for A1 and D ′D3-A1 binding to GpIbα were fit to a 1:1 interaction model. Solid lines indicate experimental data and dotted lines are model fits. C, Following GpIbα-Fc-His immobilization, 1600 nmol/L A1 and D′D3-A1 were serially injected. Binding was seen in the sensorgram (solid lines). Following this, the anti-GpIbα blocking mAb (AK-2) was injected and this bound immobilized GpIbα-Fc. Subsequent injection of VWF A1 and D′D3-A1 did not result in binding to GpIbα-Fc (dashed lines). Data are representative of 3 repeats. SPR indicates surface plasma resonance; VWF, Von Willebrand Factor.

on constructs lacking the D′D3 domain. Upon quantifying translocation velocity (Figure 6B), platelets exhibited low/negligible motion on ΔD′D3NFP^{-}-VWF and ΔD′D3OG^{-}-VWF bearing substrates at 1 dyn/cm^2. The rolling velocity on these surfaces increased at higher shear stresses, though it was typically lower compared with ΔD′D3-VWF, ΔPro-VWF and pVWF. A minimum in the translocation velocity plot upon increasing shear was noted primarily for pVWF and ΔPro-VWF, and also for ΔD′D3-VWF. This was absent upon either NFP or O-glycan deletion. Platelet accumulation was maximum and translocation velocity was minimum on ΔD′D3OG^{-}-VWF substrates at all shear stresses. In controls, cell adhesion under all conditions was blocked by mAb AK-2 (Figure 6C).

Overall, the data suggest a role for the D′D3 domain, the NFP and the O-glycans on the NFP in regulating platelet translocation. Interestingly, both N-terminal deglycosylation and NFP deletion were equally effective at augmenting

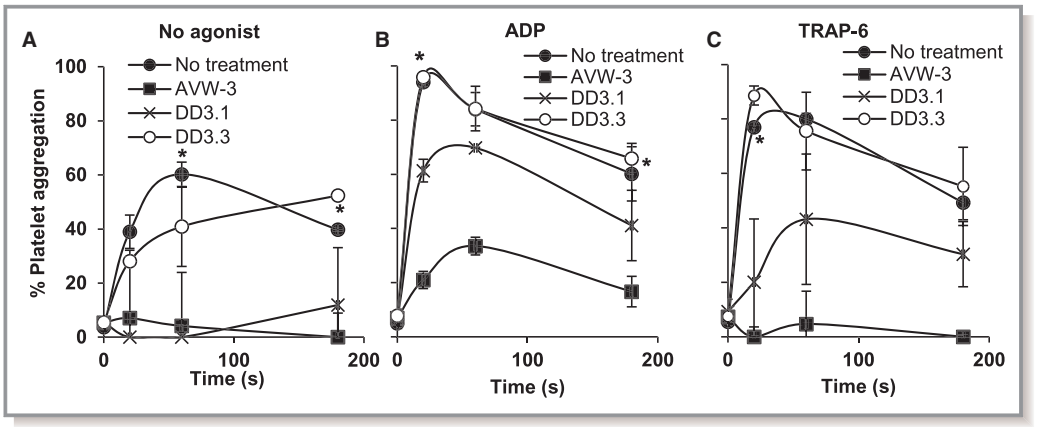

Figure 4. Blocking of platelet aggregation by anti-D′D3 mAb DD3.1. 10^8/mL CD31 labeled platelets in plasma were incubated with 100 μg/mL anti-D′D3 mAbs (DD3.1 or DD3.3) or 20 μg/mL anti-VWF-A1 domain mAb (AVW-3) for 10 minutes prior to shear application at 9600 s^{-1} in a viscometer. Platelet aggregation was measured (A) in the absence of agonists, and in the presence of (B) 0.5 μmol/L ADP or (C) 5 μmol/L TRAP-6. MAb DD3.1 reduced platelet aggregation with respect to no treatment control in all cases (*P<0.05 for no treatment compared to run with mAb DD3.1). Data are from 3 independent experiments. ADP indicates adenosine diphosphate; TRAP, thrombin receptor activating hexapeptide; VWF, Von Willebrand Factor.

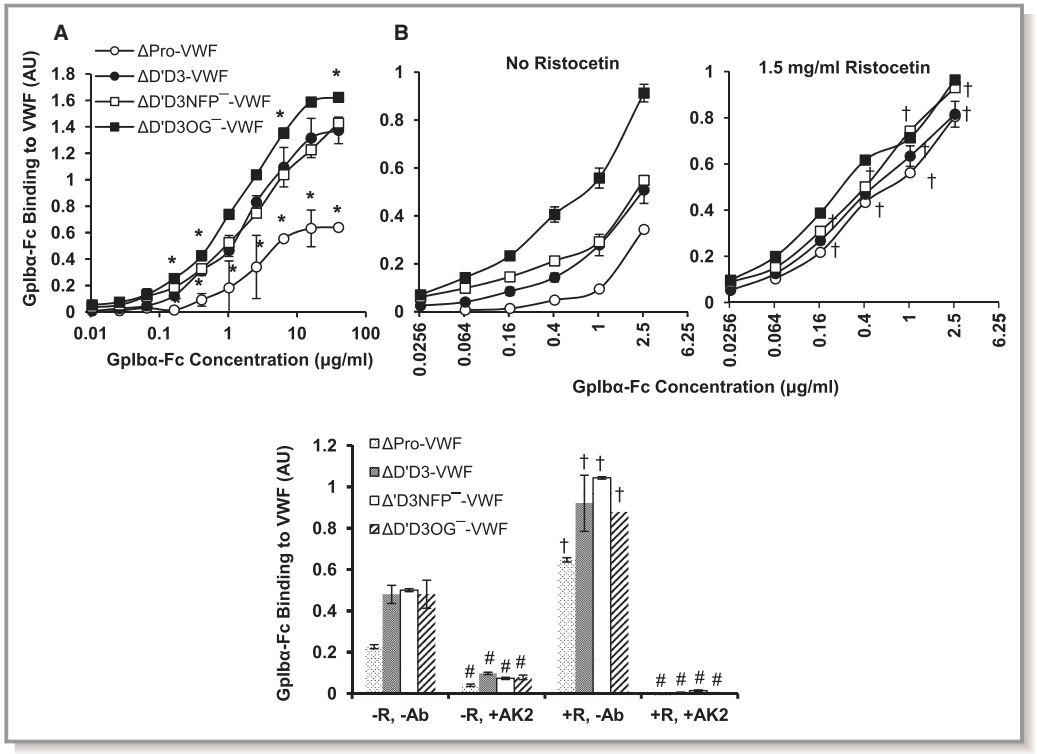

Figure 5. GpIbα-Fc binding to immobilized VWF. 4 μg/mL VWF variants were immobilized in wells. GpIbα-Fc was added in the absence or presence of ristocetin. A, GpIbα-Fc (0.01 to 100 μg/mL) binding to immobilized VWF in the absence of ristocetin. K_D values were estimated using Scatchard analysis. B, Effect of 1.5 mg/mL ristocetin on GpIbα-Fc binding to immobilized VWF. C, 4 μg/mL GpIbα-Fc added to wells bearing immobilized VWF proteins either in the absence or presence of 1.5 mg/mL ristocetin (−R or +R) or 20 μg/mL blocking antibody (−AB=no antibody; +AK2=anti-GpIbα mAb AK2). *, † and # denote $P<0.05$ with respect to all other treatments (A), no ristocetin (B and C) and no blocking antibody control (C), respectively. In (B), ristocetin increased binding of all dimeric VWF constructs except ΔD'D3OG¯-VWF ($^{\dagger}P<0.05$). Data are representative of 3 to 4 independent runs, each having 2 to 3 repeats. Error bars are too small to be visible in many cases. NFP indicates N-terminal flanking peptide; OG, O-glycans; VWF, Von Willebrand Factor.

platelet adhesion. In both cases, platelet accumulation decreased monotonically upon increasing shear.

Maximal Thrombus Formation Upon NFP Deglycosylation

Human washed platelets were reconstituted with erythrocytes at physiological hematocrit and 10 μg/mL of various recombinant dimeric VWF variants. This mixture was perfused in a flow chamber over immobilized collagen to measure thrombus formation. Studies were performed at low (wall shear rate=100/s, shear stress≈4 dyn/cm^2), moderate (250/s, 10 dyn/cm^2), and high (1000/s, 40 dyn/cm^2) fluid shear conditions. Under these conditions, the binding of ΔD′D3NFP¯-VWF to collagen was higher than other protein constructs (Figure S7) and this is in agreement with prior studies by others.[25] Here, consistent with the platelet rolling and ELISA studies, platelet substrate coverage varied as ΔPro-VWF<ΔD′D3-VWF<ΔD′D3NFP¯-VWF<ΔD′D3OG¯-VWF (Figures 7A and 7B). Whereas, experiments with ΔPro-VWF resulted in individual or small clusters of platelets bound to the substrate, large contiguous thrombi were commonly associated with ΔD′D3OG¯-VWF, especially at 1000/s. Thrombus growth on ΔD′D3NFP¯-VWF was comparable with that of ΔD′D3-VWF at the highest shears suggesting that the enhanced protein binding to collagen via VWF-A1 may somewhat reduce recognition of platelet GpIbα. Negligible platelet deposition was observed in the control lacking VWF in all experimental runs.

Discussion

The study evaluated the relative roles of the VWF-D′D3 domain, A1 N-terminal flanking peptide and O-glycans on this peptide in controlling VWF-A1 GpIbα binding. Particular emphasis was placed on studies under fluid shear, and the distinction between the structural features controlling VWF

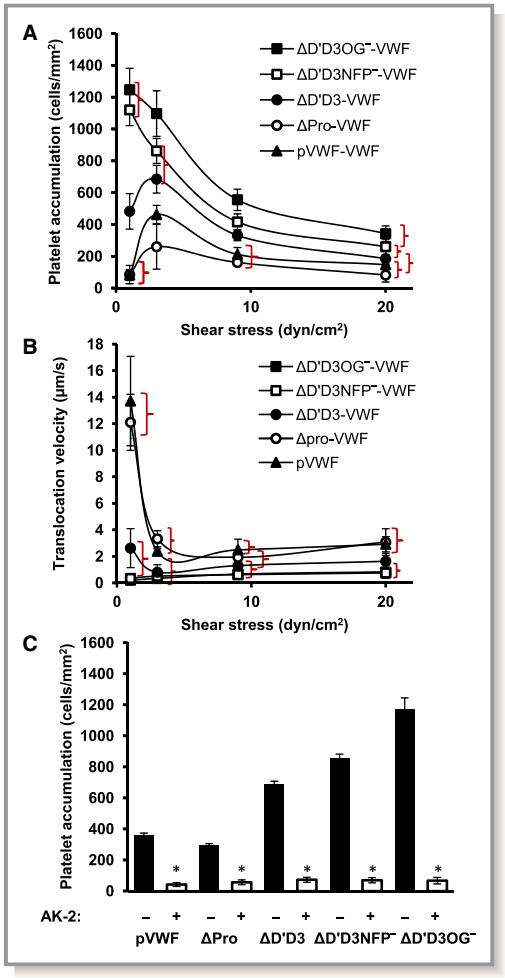

Figure 6. Platelet binding to pVWF and VWF variants. 10^8/mL washed platelets were perfused over VWF bearing substrates at varying fluid shear stresses. A, Platelet accumulation was quantified 2 minutes after the start of perfusion. B, Platelet translocation velocity. In A and B, all treatments at a given shear were different from each other except for those enclosed within curly brackets ($P<0.05$). C, Anti-GpIbα blocking mAb AK-2 was incubated with washed platelets for 10 minutes prior to platelet perfusion at 3 dyn/cm^2. *$P<0.05$ with respect to corresponding run lacking AK-2. Data from 4 independent experiments. NFP indicates N-terminal flanking peptide; OG, O-glycans; pVWF, plasma Von Willebrand Factor.

binding onto platelets from solution, versus immobilized VWF capture of platelets from flow.

The VWF-D′D3 Domain

The data demonstrate that VWF-D′D3 plays a substantial role in inhibiting both soluble and immobilized VWF binding to platelet GpIbα under shear flow. Consistent with this, the apparent K_D of soluble ΔPro-VWF binding to GpIbα was 50- to 100-fold higher compared to other VWF constructs lacking the D′D3-domain. No major difference was observed among the proteins lacking VWF-D′D3, except that the K_D of soluble ΔD′D3NFP$^-$-VWF was 1/3rd that of ΔD′D3-VWF and ΔD′D3OG$^-$-VWF suggesting a minor role for the NFP. Additionally, an anti-D′D3 antibody (DD3.1) blocked SIPA in the presence of endogenous multimeric VWF at high shear stress, and this confirms that the juxtapositioning of the A1- and D′D3-domains is a key feature regulating soluble protein binding. SIPA studies were not performed with dimeric VWF variants since this assay requires multimeric proteins. Consistent with our functional data, the physical proximity between VWF-A1 and the irregularly shaped D′D3-domain under physiological pH is also evident using negative stain electron microscopy.[26] More recently, these authors have also extended their electron microscopy studies to provide a more complete annotation of the VWF protein including designating the original D3 domains to contain an "assembly" of smaller lobes that include the VWD, Cysteine 8 (C8), trypsin-inhibitor-like (TIL), and "E" modules.[2] The D' domain also contains a TIL and E-module. The relative impact of these sub-domains on VWF-A1 function remains to be determined.

In addition to its role in reducing wild-type VWF A1-domain binding to platelet GpIbα under shear, it is possible that the molecular interaction between VWF-D′D3, NFP, and VWF-A1 may also be relevant to von Willebrand disease (VWD) especially type 2B and 2M.[1,27] In such diseases, point mutations that lie away from the GpIbα VWF-A1 binding interface and even internal to VWF-A1 contribute to either enhanced or diminished platelet adhesion. For example, several of the VWD Type 2B mutations lie proximal to the NFP of the A1-domain.[28] In some instances, similar to ΔD′D3-VWF, the enhancement of GpIbα-VWF binding affinity/kinetics upon mutation in VWD can result in premature or spontaneous platelet adhesion in regions of low fluid shear. Under these conditions, it remains to be determined if certain VWD mutations alter the nature of VWF-A1 D′D3 interactions at the domain-level, thus impacting platelet-VWF binding.

The N-Terminal Peptide and O-Glycans on the NFP

It has been suggested that VWF in solution exists in a "latent", non-adhesive form and that the binding of this protein to substrate results in an "active" protein.[29] Some of our experiments support this line of reasoning.

First, the deletion of the NFP or the absence of O-glycans on this peptide augmented the binding of soluble GpIbα and platelet rolling on immobilized recombinant VWF, and also thrombus formation under shear. However, these same mutations only had a minor impact on soluble VWF binding to immobilized GpIbα. With respect to this, our results that

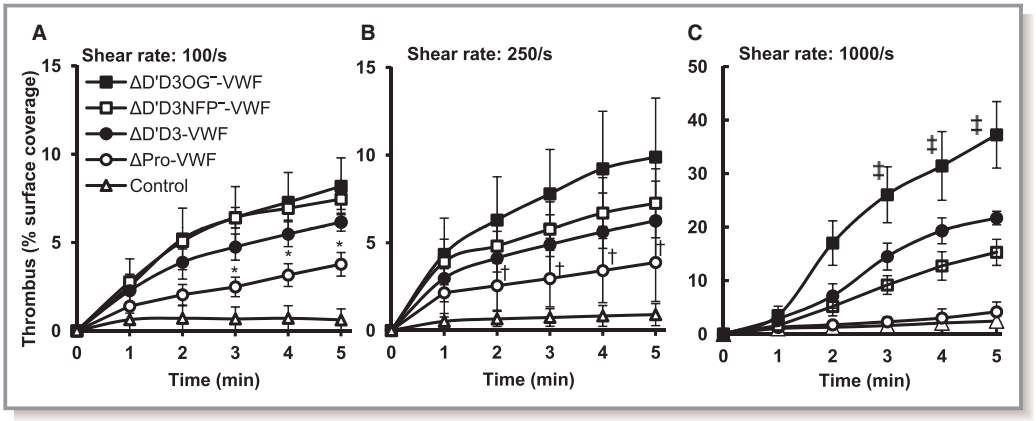

Figure 7. Platelet adhesion onto fibrillar collagen in the presence of VWF variants. 10^8 BCECF-labeled fluorescent platelets/mL were resuspended in plasma-free blood supplemented with 10 μg/mL VWF variants. This was perfused over collagen bearing substrates for 5 minutes at a wall shear rate of either: (A) 100 s^{-1}, (B) 250 s^{-1} or (C) 1000 s^{-1}. Thrombus formation quantified the % of substrate covered by platelets. Control runs were plasma-free without added VWF. *P<0.05 for ΔPro-VWF with respect to ΔD′D3-VWF, ΔD′D3NFP¯-VWF and ΔD′D3OG¯-VWF at indicated times. †P<0.05 for ΔPro-VWF with respect to ΔD′D3NFP¯-VWF and ΔD′D3OG¯-VWF. ‡P<0.05 for ΔD′D3OG¯-VWF with respect to all other constructs. Data are mean±standard deviation from 4 independent experiments. BCECF indicates 2′,7′-bis-(2-carboxyethyl)-5-(and-6)-carboxyfluorescein; NFP, N-terminal flanking peptide; OG, O-glycans; VWF, Von Willebrand Factor.

NFP deletion enhances platelet capture on immobilized VWF-A1 under flow are consistent with previous work.[8,14] The observation that NFP O-glycosylation alters VWF-A1 binding function has also been suggested.[16,17] In this regard, similar to our work, Nowak et al[17] show that NFP O-glycan removal enhances thrombus formation ex vivo. Using hydrodynamic injection of multimeric VWF variants, Badirou et al[16] show that some of the mutations (T1255A and T1256A) also enhance mouse tail bleeding times. While all reports generally note an effect of the NFP O-glycans, some differences remain that may be due to the precise manner in which the O-glycan mutations were implemented in dimeric/multimeric VWF. Overall, since NFP removal and O-glycan deletion result in similar quantitative enhancement of platelet adhesion under shear in the current work, it appears that the O-glycans on NFP may promote peptide interaction with VWF-A1. This may then reduce VWF capture of platelets under shear.

Second, the difference between ΔPro-VWF and ΔD′D3-VWF in ELISA studies that measure soluble VWF-variants binding from solution to immobilized GpIbα-Fc versus GpIbα-Fc binding to immobilized VWF is noteworthy. In this regard, the K_D of ΔPro-VWF binding to GpIbα-Fc was 102 nmol/L when VWF was in solution and ≈15 nmol/L when the VWF was immobilized. In contrast, ΔD′D3-VWF bound GpIbα-Fc with K_D≈2 to 10 nmol/L in both assays. Although not all VWF-A1 sites on ΔPro-VWF were available upon immobilization (Figure 5A), the remarkable K_D difference noted here suggests that ΔPro-VWF may change its conformation upon substrate immobilization to promote VWF-A1 GpIbα binding. The altered conformation, however, does not completely expose VWF-A1 since the ΔD′D3-VWF variants displayed more avid binding under all experimental conditions.

Third, ristocetin reproducibly inhibited soluble ΔD′D3NFP¯-VWF binding to immobilized GpIbα-Fc (Figure 2B) while it augmented soluble GpIbα-Fc binding to immobilized ΔD′D3NFP¯-VWF (Figure 5B). Thus, for this protein, the relative location of the ristocetin binding region with respect to the VWF-GpIbα "β-finger" binding interface in the solution versus substrate-immobilization assay may be different. In this regard, ΔD′D3NFP¯-VWF begins at aa1267 and it lacks the putative VWF-A1 N-terminal ristocetin binding segment (aa1238 to 1251).[23] Based on the current work, it appears that ristocetin can interact with VWF-A1 even in the absence of this segment. Additionally, it may also dimerize and bind GpIbα, thus further augmenting VWF-A1 recognition.[30] Due to this, deletion of specific N-terminal flanking peptide segments[28] and single-nucleotide polymorphisms in the VWF-A1 overhang peptides[31] may result in substantially different responses in ristocetin and platelet-based functional assays.

Platelet Adhesion Under Hydrodynamic Shear

Platelet translocation on immobilized VWF is a complex process that is regulated by: (1) hydrodynamic phenomena that control the number and nature of GpIbα contacts with VWF-A1 at the binding interface,[32–35] (2) conformation changes in VWF,[36–39] and (3) the biophysical nature of the

VWF-A1 GpIbα bond.[40,41] In this context, our ELISA and cell adhesion studies suggest that immobilized VWF may exist in 3 distinct functional forms. First, immobilized ΔPro-VWF and pVWF exist in a partially active form where a subset of the protein can engage GpIbα. This protein could not recruit platelets at low fluid shear stresses (1 dyn/cm^2), but was functional at higher shears. Based on SPR studies, the high K_D (≈1.5 μmol/L), on-rate (1.8×10^4 (mol/L)$^{-1}\cdot$s^{-1}) and off-rate (0.088/s) of native VWF binding to GpIbα may be optimized for weak cellular interactions in blood. At higher stresses, platelet deformation may enhance the number of GpIbα receptors in the flattened interfacial area between the platelet and VWF,[42] thus enhancing the ability of platelets to resist the higher hydrodynamic drag forces.[7,34] Second, deletion of the VWF-D′D3 domain resulted in a moderately active protein. This modification restored platelet adhesion at 1 dyn/cm^2 presumably by enhancing the on-rate of VWF-A1 GpIbα binding to 5.1×10^4 (mol/L)$^{-1}\cdot$s^{-1} as measured using SPR. At this shear, platelet translocation on ΔD′D3-VWF resulted in more tethering/recruitment events and lower translocation velocities compared to substrates composed of either ΔPro-VWF or pVWF. Reinforcing this importance for VWF-D′D3 the anti-D′D3 mAb DD3.1, which inhibited SIPA in this study, was also previously shown to block thrombus formation on collagen under flow.[9] Third, deletion of the NFP or O-glycan removal resulted in a hyper-adhesive VWF. Thus, platelet recruitment on ΔD′D3NFP$^-$-VWF and ΔD′D3OG$^-$-VWF resulted in extremely low translocation velocities at all shears. Similar rolling data were reported previously using single A1-domain constructs lacking the NFP.[43] The affinity of ΔD′D3OG$^-$-VWF binding to GpIbα-Fc was also only marginally enhanced by ristocetin suggesting that this protein is maximally active.

In summary, the data provide strong evidence that the VWF D′D3-domain plays a key role in reducing VWF-A1 binding interaction with platelet GpIbα under hydrodynamic shear. An addition role for the peptide segment N-terminal to the A1-domain and the O-glycans on this peptide is evident, particularly in the platelet translocation and thrombus formation assays. These features likely represent important control mechanisms that control platelet recruitment at sites of vascular injury both under physiological and pathological flow conditions. It is important to note that while the above conclusions are based on studies with full-length dimeric human VWF protein, additional validation of this concept is necessary using the multimeric form of VWF.

Sources of Funding

AHA pre-doctoral fellowship (to Madabhushi), and NIH grants HL103411 and HL77258 (to Neelamegham).

Disclosures

None.

References

1. Sadler JE. Biochemistry and genetics of von Willebrand factor. *Annu Rev Biochem*. 1998;67:395–424.
2. Zhou YF, Eng ET, Zhu J, Lu C, Walz T, Springer TA. Sequence and structure relationships within von Willebrand factor. *Blood*. 2012;120:449–458.
3. Ikeda Y, Handa M, Kawano K, Kamata T, Murata M, Araki Y, Anbo H, Kawai Y, Watanabe K, Itagaki I. The role of von Willebrand factor and fibrinogen in platelet aggregation under varying shear stress. *J Clin Invest*. 1991;87:1234–1240.
4. Shankaran H, Alexandridis P, Neelamegham S. Aspects of hydrodynamic shear regulating shear-induced platelet activation and self-association of von Willebrand factor in suspension. *Blood*. 2003;101:2637–2645.
5. Girdhar G, Bluestein D. Biological effects of dynamic shear stress in cardiovascular pathologies and devices. *Expert Rev Med Devices*. 2008;5:167–181.
6. Alevriadou BR, Moake JL, Turner NA, Ruggeri ZM, Folie BJ, Phillips MD, Schreiber AB, Hrinda ME, McIntire LV. Real-time analysis of shear-dependent thrombus formation and its blockade by inhibitors of von Willebrand factor binding to platelets. *Blood*. 1993;81:1263–1276.
7. Savage B, Saldivar E, Ruggeri ZM. Initiation of platelet adhesion by arrest onto fibrinogen or translocation on von Willebrand factor. *Cell*. 1996;84:289–297.
8. Auton M, Sowa KE, Behymer M, Cruz MA. N-terminal flanking region of A1 domain in von Willebrand factor stabilizes structure of A1A2A3 complex and modulates platelet activation under shear stress. *J Biol Chem*. 2012;287:14579–14585.
9. Madabhushi SR, Shang C, Dayananda KM, Rittenhouse-Olson K, Murphy M, Ryan TE, Montgomery RR, Neelamegham S. Von Willebrand factor (VWF) propeptide binding to VWF D'D3 domain attenuates platelet activation and adhesion. *Blood*. 2012;119:4769–4778.
10. Nishio K, Anderson PJ, Zheng XL, Sadler JE. Binding of platelet glycoprotein Ibalpha to von Willebrand factor domain A1 stimulates the cleavage of the adjacent domain A2 by ADAMTS13. *Proc Natl Acad Sci USA*. 2004;101:10578–10583.
11. Ulrichts H, Udvardy M, Lenting PJ, Pareyn I, Vandeputte N, Vanhoorelbeke K, Deckmyn H. Shielding of the A1 domain by the D'D3 domains of von Willebrand factor modulates its interaction with platelet glycoprotein Ib-IX-V. *J Biol Chem*. 2006;281:4699–4707.
12. Huizinga EG, Tsuji S, Romijn RA, Schiphorst ME, de Groot PG, Sixma JJ, Gros P. Structures of glycoprotein Ibalpha and its complex with von Willebrand factor A1 domain. *Science*. 2002;297:1176–1179.
13. Dumas JJ, Kumar R, McDonagh T, Sullivan F, Stahl ML, Somers WS, Mosyak L. Crystal structure of the wild-type von Willebrand factor A1-glycoprotein Ib-alpha complex reveals conformation differences with a complex bearing von Willebrand disease mutations. *J Biol Chem*. 2004;279:23327–23334.
14. Ju L, Dong JF, Cruz MA, Zhu C. The N-terminal flanking region of the A1 domain regulates the force-dependent binding of von Willebrand factor to platelet glycoprotein Ibalpha. *J Biol Chem*. 2013;288:32289–32301.
15. Titani K, Kumar S, Takio K, Ericsson LH, Wade RD, Ashida K, Walsh KA, Chopek MW, Sadler JE, Fujikawa K. Amino acid sequence of human von Willebrand factor. *Biochemistry*. 1986;25:3171–3184.
16. Badirou I, Kurdi M, Legendre P, Rayes J, Bryckaert M, Casari C, Lenting PJ, Christophe OD, Denis CV. In vivo analysis of the role of O-glycosylations of von Willebrand factor. *PLoS One*. 2012;7:e37508.
17. Nowak AA, Canis K, Riddell A, Laffan MA, McKinnon TA. O-linked glycosylation of von Willebrand factor modulates the interaction with platelet receptor glycoprotein Ib under static and shear stress conditions. *Blood*. 2012;120:214–222.
18. Buffone A Jr, Mondal N, Gupta R, McHugh KP, Lau JT, Neelamegham S. Silencing alpha1,3-fucosyltransferases in human leukocytes reveals a role for FUT9 enzyme during E-selectin-mediated cell adhesion. *J Biol Chem*. 2013;288:1620–1633.
19. Singh I, Shankaran H, Beauharnois ME, Xiao Z, Alexandridis P, Neelamegham S. Solution structure of human von Willebrand factor studied using small angle neutron scattering. *J Biol Chem*. 2006;281:38266–38275.
20. Dayananda KM, Singh I, Mondal N, Neelamegham S. Von Willebrand factor self-association on platelet Gplbalpha under hydrodynamic shear: effect on shear-induced platelet activation. *Blood*. 2010;116:3990–3998.

21. Coburn LA, Damaraju VS, Dozic S, Eskin SG, Cruz MA, McIntire LV. GpIbalpha-VWF rolling under shear stress shows differences between type 2B and 2M von Willebrand disease. *Biophys J*. 2011;100:304–312.
22. Mohri H, Fujimura Y, Shima M, Yoshioka A, Houghten RA, Ruggeri ZM, Zimmerman TS. Structure of the von Willebrand factor domain interacting with glycoprotein Ib. *J Biol Chem*. 1988;263:17901–17904.
23. Sadler JE. Redeeming ristocetin. *Blood*. 2010;116:155–156.
24. Lo CY, Antonopoulos A, Gupta R, Qu J, Dell A, Haslam SM, Neelamegham S. Competition between core-2 GlcNAc-transferase and ST6GalNAC-transferase regulates the synthesis of the leukocyte selectin ligand on human P-selectin glycoprotein ligand-1. *J Biol Chem*. 2013;288:13974–13987.
25. Bonnefoy A, Romijn RA, Vandervoort PA, Van Rompaey I, Vermylen J, Hoylaerts MF. Von Willebrand factor A1 domain can adequately substitute for A3 domain in recruitment of flowing platelets to collagen. *J Thromb Haemost*. 2006;4:2151–2161.
26. Zhou YF, Eng ET, Nishida N, Lu C, Walz T, Springer TA. A pH-regulated dimeric bouquet in the structure of von Willebrand factor. *EMBO J*. 2011;30:4098–4111.
27. Lillicrap D. Von Willebrand disease: advances in pathogenetic understanding, diagnosis, and therapy. *Blood*. 2013;122:3735–3740.
28. Nakayama T, Matsushita T, Dong Z, Sadler JE, Jorieux S, Mazurier C, Meyer D, Kojima T, Saito H. Identification of the regulatory elements of the human von Willebrand factor for binding to platelet GPIb. Importance of structural integrity of the regions flanked by the CYS1272-CYS1458 disulfide bond. *J Biol Chem*. 2002;277:22063–22072.
29. Groot E, de Groot PG, Fijnheer R, Lenting PJ. The presence of active von Willebrand factor under various pathological conditions. *Curr Opin Hematol*. 2007;14:284–289.
30. Hoylaerts MF, Nuyts K, Peerlinck K, Deckmyn H, Vermylen J. Promotion of binding of von Willebrand factor to platelet glycoprotein Ib by dimers of ristocetin. *Biochem J*. 1995;306(Pt 2):453–463.
31. Flood VH, Gill JC, Morateck PA, Christopherson PA, Friedman KD, Haberichter SL, Branchford BR, Hoffmann RG, Abshire TC, Di Paola JA, Hoots WK, Leissinger C, Lusher JM, Ragni MV, Shapiro AD, Montgomery RR. Common VWF exon 28 polymorphisms in African Americans affecting the VWF activity assay by ristocetin cofactor. *Blood*. 2010;116:280–286.
32. Zhang Y, Neelamegham S. Estimating the efficiency of cell capture and arrest in flow chambers: study of neutrophil binding via E-selectin and ICAM-1. *Biophys J*. 2002;83:1934–1952.
33. Mody NA, Lomakin O, Doggett TA, Diacovo TG, King MR. Mechanics of transient platelet adhesion to von Willebrand factor under flow. *Biophys J*. 2005;88:1432–1443.
34. Shankaran H, Neelamegham S. Hydrodynamic forces applied on intercellular bonds, soluble molecules, and cell-surface receptors. *Biophys J*. 2004;86:576–588.
35. Nesbitt WS, Westein E, Tovar-Lopez FJ, Tolouei E, Mitchell A, Fu J, Carberry J, Fouras A, Jackson SP. A shear gradient-dependent platelet aggregation mechanism drives thrombus formation. *Nat Med*. 2009;15:665–673.
36. Siedlecki CA, Lestini BJ, Kottke-Marchant KK, Eppell SJ, Wilson DL, Marchant RE. Shear-dependent changes in the three-dimensional structure of human von Willebrand factor. *Blood*. 1996;88:2939–2950.
37. Schneider SW, Nuschele S, Wixforth A, Gorzelanny C, Alexander-Katz A, Netz RR, Schneider MF. Shear-induced unfolding triggers adhesion of von Willebrand factor fibers. *Proc Natl Acad Sci USA*. 2007;104:7899–7903.
38. Singh I, Themistou E, Porcar L, Neelamegham S. Fluid shear induces conformation change in human blood protein von Willebrand factor in solution. *Biophys J*. 2009;96:2313–2320.
39. Themistou E, Singh I, Shang C, Balu-Iyer SV, Alexandridis P, Neelamegham S. Application of fluorescence spectroscopy to quantify shear-induced protein conformation change. *Biophys J*. 2009;97:2567–2576.
40. Yago T, Lou J, Wu T, Yang J, Miner JJ, Coburn L, Lopez JA, Cruz MA, Dong JF, McIntire LV, McEver RP, Zhu C. Platelet glycoprotein Ibalpha forms catch bonds with human WT VWF but not with type 2B von Willebrand disease VWF. *J Clin Invest*. 2008;118:3195–3207.
41. Kim J, Zhang CZ, Zhang X, Springer TA. A mechanically stabilized receptor-ligand flex-bond important in the vasculature. *Nature*. 2010;466:992–995.
42. Bose S, Das SK, Karp JM, Karnik R. A semianalytical model to study the effect of cortical tension on cell rolling. *Biophys J*. 2010;99:3870–3879.
43. Tischer A, Cruz MA, Auton M. The linker between the D3 and A1 domains of vWF suppresses A1-GPIbalpha catch bonds by site-specific binding to the A1 domain. *Protein Sci*. 2013;22:1049–1059.